

## ORIGINAL RESEARCH

### Strategic lyophilization of rhamnolipid-modified niclosamide liposomes for enhanced solubility and regulated drug release

Sujit A Desai<sup>a\*</sup>, Himanshu Paliwal<sup>b</sup>, Sachin S Mali<sup>c</sup>, Anbhule Sachin Jalindar<sup>d</sup>, Arehalli Manjappa<sup>e</sup>, Durgacharan A Bhagwat<sup>c</sup>, Sudarshan Singh<sup>f,g\*</sup>, Bhupendra G. Prajapati<sup>h</sup>

<sup>a</sup> Department of Pharmaceutics, Department of Pharmaceutics, School of Pharmacy and Research Centre Baramati, Maharashtra 413115, India

<sup>b</sup> Marwadi University Research Center, Faculty of Pharmacy, Marwadi University, Rajkot, Gujarat, 360003, India

<sup>c</sup> Department of Pharmaceutics, Bharati Vidyapeeth college of Pharmacy, Kolhapur Maharashtra 416013, India

<sup>d</sup> HSBPVT's, GOI, Faculty of Pharmacy, Shrigonda, Ahilyanagar, Maharashtra 413701, India

<sup>e</sup> Department of Pharmaceutics, Vasantidevi Patil Institute of Pharmacy, Kodoli, Kolhapur Maharashtra 416113, India

<sup>f</sup> Office of Research Administrations, Chiang Mai University, Chiang Mai, 50200, Thailand

<sup>g</sup> Faculty of Pharmacy, Chiang Mai University, Chiang Mai, 50200, Thailand

<sup>h</sup> Department of Pharmaceutics, Parul Institute of Pharmacy, Faculty of Pharmacy, Parul University, Waghdoda, Vadodara, 391760, Gujarat, India

**Corresponding Author's Email:** [sudarshan.s@cmu.ac.th](mailto:sudarshan.s@cmu.ac.th) and [sujitdesai37@gmail.com](mailto:sujitdesai37@gmail.com)

(\*Both authors have equal contribution)

© The Author(s), 2025

#### Abstract

Niclosamide (NSD) is a widely known anthelmintic agent that has garnered attention in recent times due to its therapeutic potential in metabolic, viral, and oncological disorders. Although its clinical translation continues to be restricted owing to low aqueous solubility and poor bioavailability. The study is focused on developing and optimizing rhamnolipid-modified liposomes loaded with niclosamide for enhancing the solubility, stability, and release profile. The liposomes were formulated by the thin-film hydration method, and Box-Behnken Design was used for optimizing concentrations of hydrogenated soy phosphatidylcholine (HSPC), cholesterol, and soybean oil. The optimized formulation showed high drug content (80.94 %) and a small vesicle size (149.2 nm), with a polydispersity index of 0.261 and a zeta potential of  $-14.2\text{ mV}$ , suggesting uniformity and stability. The structural (FTIR) and XRD studies exhibited drug integrity and amorphization, whereas thermal (DSC) suggested a reduction in crystallization after incorporation into liposomes. The sustained release behaviour of NSD from the liposomal formulation was observed in drug release studies. Stability analysis showed an insignificant reduction in entrapment efficiency, verifying the robustness of the formulation. Overall, the outcomes of the study exhibit a novel lipid-based delivery system that considerably improves NSD sustained release behaviour and stability, presenting a potential approach for enhancing therapeutic effectiveness, whereas evading the limitations of traditional formulations.

**Keywords:** Niclosamide; Liposomes; Rhamnolipids; Box–Behnken design; Drug delivery; Sustained release

#### Article History:

**Received:** 28-Aug-2025

**Revised:** 20-Nov-2025

**Accepted:** 07-Dec-2025

**Published:** 23-Dec-2025

## 1. Introduction

Niclosamide (NSD) is an anthelminthic drug for oral use that has garnered interest for its probable utilization as an anti-obesity drug and decreased cholesterol levels, commonly prescribed in conjunction with a nutritious diet, consistent physical activity, and endeavours to shed excess weight (Al-Gareeb et al., 2017; Singh et al., 2017; Unnisa et al., 2023; Yadav et al., 2020). The NSD works by uncoupling oxidative phosphorylation, contributing to stimulation of adenosine triphosphatase activity in the mitochondria. The mitochondria have the primary function of generating energy from nutrients as adenosine triphosphate (ATP), and an increase in oxidation of lipid via mitochondria may lessen the lipid accumulated in the cells (Nassir & Ibdah, 2014). The characteristic feature of mitochondrial uncoupling by NSD is the stimulation of mitochondrial oxygen utilization, despite the availability of ATP synthase inhibitors like oligomycin (Al-Gareeb et al., 2017; Singh et al., 2017). Niclosamide has great potential for dealing with obesity, but it poses a lot of problems that make it challenging for clinical translation. Such challenges are mainly ascribed to the drug's low water solubility (0.23 µg/mL) and categorized under the Biopharmaceutical Classification System (BCS) Class II. Apart from low solubility in water, it exhibits faster metabolism in the liver and intestine (Bhalani et al., 2022; Fan et al., 2019). Niclosamide's hydrophobic nature strongly restricts its absorption in the gastrointestinal tract, whereas its faster clearance via cytochrome P450-mediated hydroxylation and glucuronidation lowers its systemic availability (Ju & Zhang, 2021; Mast et al., 2021). The pharmacokinetic obstacles contribute to subtherapeutic plasma concentrations, requiring higher doses, which pose challenges in clinical sustenance of such a therapy and also increase in chances of side effects.

Owing to these limitations, there is an obvious requirement for novel formulations and delivery strategies for improving therapeutic outcomes. The approaches for enhancing bioavailability, like the fabrication of NSD derivatives via O-alkylation and halogenation, have shown promise in enhancing solubility and bioavailability (Chen et al., 2013; He et al., 2021; Mito et al., 2023). Different strategies, such as polymeric nanoparticles, cyclodextrin complexes, etc., have also exhibited the capacity to enhance the efficiency of delivery and drug stability (Jain et al., 2019; Lodagekar et al., 2019; Lourith & Kanlayavattanakul, 2009).

Lipid-based nanocarrier systems are one of the alternatives that are being investigated for their capacity to enhance the pharmacokinetic profile of NSD along with targeted delivery (Luo et al., 2019). These attempts are focused on maintaining the anti-obesity and cholesterol-reducing potency of NSD while evading the pharmacological barrier that restricts its therapeutic effectiveness. Liposomes form concentric lipid layers around the therapeutic agent, which improves their solubility in the aqueous environment and enhances the circulation time of the drug (Mohite et al., 2023). These lipid nanocarriers also enable the loading of the compounds, which results in the enhancement of pharmacokinetic and pharmacodynamic features of the drug, which facilitates higher accumulation at the tumor site while lowering systemic toxicity (Singh, Supaweera, Nwabor, Chaichompoo, et al., 2024; Singh, Supaweera, Nwabor, Yusakul, et al., 2024).

Biosurfactants are one of those types of surfactants that are produced by specific types of microbes (Das et al., 2008). Rhamnolipids are among the extensively utilized biosurfactants, specifically generated commercially by microbial fermentation employing strains, like *Pseudomonas* (Kosaric & Sukan, 2014). The comprises a hydrophilic glycosyl head group, called rhamnose, and a lipophilic 3-(hydroxyalk-anoxyloxy) alkanoic fatty acid

tail (Kosaric & Sukan, 2014). Such a biosurfactant has gained a lot of interest for various commercial applications owing to its eco-friendliness, low toxicity, and biodegradability in comparison with different synthetic surfactants. Furthermore, they can function over a wide variety of environmental settings, and can be generated from renewable sources, industrial waste, and by-products. Owing to the probable advantages of using rhamnolipids, they have been explored for application in a variety of industries, including foods (Nitschke & Costa, 2007), pharmaceuticals (Yi et al., 2019), cosmetics (Lourith & Kanlayavattanakul, 2009), agriculture (Sachdev & Cameotra, 2013), and environmental applications (Mali et al., 2025; Mulligan, 2009). Recently, the ability of rhamnolipids to improve the physical stability and efficacy of diverse colloidal systems were investigated, such as emulsions (Cheng et al., 2019; Haba et al., 2014) and nanoparticles (Müller et al., 2017). Moussa *et al* originally characterized membrane fluidity, partition coefficient, permeability, and phase transition temperature to examine how the rhamnolipids at low doses interact with the phospholipid membrane that could enhance NSD stability at neutral and alkaline buffer settings (Moussa et al., 2017).

In comparison with conventional nanocarriers, the rhamnolipid-modified liposomal strategy provides unique benefits. The utilization of natural biosurfactant enhances the amphiphilicity and membrane fluidity of the vesicles, which results in efficient encapsulation of niclosamide, enhanced aqueous dispersibility, and decreased dependence on synthetic surfactants that may lead to irritation or toxicity. Furthermore, this approach improves the stability of formulation and offers a biocompatible and eco-friendly option adequate for prolonged therapeutic application (Hsu et al., 2025; Plaza-Oliver et al., 2021; Sanches et al., 2021). This study is aimed at preparing rhamnolipid-modified liposomes by means of the thin film hydration method. This modification of the liposomes will improve stability to the liposomes, and their physicochemical features were estimated by examining vesicle size, zeta-potential, and morphology. The drug loading property of liposomes was assessed by estimating the entrapment efficiency and loading capacity. Furthermore, the *in vitro* release profile and stability of optimized liposomes were also studied in the study.

## 2. Materials and Methods

### 2.1. Materials

Niclosamide was acquired from Sigma Aldrich (Mumbai, India). Cholesterol was acquired from HiMedia (Bangalore, India), whereas Hydrogenated soy phosphatidylcholine (HSPC) was provided by Lipoid GmbH (Ludwigshafen, Germany). Rhamnolipids were procured from Xi'an boliant Chemical Co. (Xi'an, China). The soybean oil was procured from Molychem (Mumbai, India). Other reagents employed in the research were of analytical grade.

### 2.2. Preparation and optimization of NSD-Liposomes

The NSD-loaded liposomes (NSD-LPs) were created by the thin-film hydration method as described previously (Isailović et al., 2013; Jangde & Singh, 2016) with slight modifications. In summary, the HSPC, Cholesterol, soybean oil, and drug were dissolved in a 15 mL solution of methanol and chloroform in a 1:2 volume-to-volume ratio employing bath sonication. The solvent was volatilized at a temperature of  $65 \pm 2$  °C by utilizing a rotary evaporator (BUCHI Rotavapor R-200, BUCHI India Private Ltd, India) in order to produce a thin layer, which was subsequently subjected to a vacuum overnight to remove any leftover solvent. Hydration of the film was done

using sterile water for injection at a temperature of  $70 \pm 2$  °C for a duration of 15 min. The size of multilamellar liposomes was decreased using probe sonication, resulting in the formation of small unilamellar vesicles. This process involved 5 cycles of sonication, with each cycle lasting for 1 minute. Each cycle has a duration of 12 seconds during which the electrical system operates at a voltage of 240V and a current of 0.6A, followed by a subsequent duration of 8 seconds during which the system is inactive. The film that contained water was subjected to sonication using a probe sonicator, which involved alternating cycles of heating. To modify the liposomes, the required quantity of rhamnolipid was first dissolved in 1 mL of methanol, followed by heating it on a water bath at 60 °C until a film was formed. This was followed by the incorporation of purified liposomes into the respective films. The heating of the solutions was done using a water bath at 70°C using by rotary evaporator to facilitate appropriate coating of the liposomes.

### 2.3. Experimental design

The optimization of the formulation variables and assessment of the single, interaction, and quadratic effects of the formulation components on the performance of NSD-LPs was carried out using Box-Behnken Design (BBD) (Mohite et al., 2025; Panchal et al., 2025). The three-factor, three-level experimental design was chosen for evaluating quadratic responses and generating a suitable polynomial model using Design Expert® software (Trial Version 13, Stat-Ease Inc., Minneapolis, MN). BBD was chosen over other response surface designs as it requires a comparatively smaller number of runs. The design is characterized by experimental points located at the midpoints of the edges of a multidimensional cube, and replications ( $n = 5$ ) of centre points were taken to improve precision. The corresponding non-linear quadratic models are shown as:

Where  $Y_i$  is the estimated response,  $\beta_0$  is an intercept, and  $\beta_1$  and  $\beta_2$  are measured regression coefficients calculated from the experimental response values.  $X_1$  and  $X_2$  represent individual main effect terms;  $X_1X_2$  are the interaction terms, and  $X_1^2$  and  $X_2^2$  indicate the quadratic terms. The dependent and independent variables selected for the NSD-LPs are indicated in Table 1. The multivariate optimization approach discovered three distinct factors: HSPC ( $X_1$ ), cholesterol ( $X_2$ ), and soybean oil ( $X_3$ ). The measured responses were the entrapment efficiency ( $Y_1$ ) and the particle size ( $Y_2$ ). A design matrix with 17 experimental runs was generated as indicated in Table 2.

**Table 1.** Independent variables at three levels and responses utilized for the Box-Behnken Design.

Independent variables	Low (-1)	Medium (0)	High (+1)
X <sub>1</sub> - HSPC (mg)	33.25	50.76	68.26
X <sub>2</sub> - Cholesterol (mg)	8.65	39.78	70.91
X <sub>3</sub> - Soyabean oil (mg)	5.58	26.42	47.26
Dependent variables (Factors)			
Y <sub>1</sub> - Drug content (%) - Maximum			
Y <sub>2</sub> - Vesicle size (nm) – Minimum			

**Table 2.** Design matrix of NSD-loaded liposomes as per BBD.

Runs	HSPC (X <sub>1</sub> ) mg	Cholesterol (X <sub>2</sub> ) mg	Soyabean oil (X <sub>3</sub> ) mg
1	33.25	8.65	26.42
2	68.26	8.65	26.42
3	33.25	70.91	26.42
4	68.26	70.91	26.42
5	33.25	39.78	5.58
6	68.26	39.78	5.58
7	33.25	39.78	47.26
8	68.26	39.78	47.26
9	50.76	8.65	5.58
10	50.76	70.91	5.58
11	50.76	8.65	47.26
12	50.76	70.91	47.26
13	50.76	39.78	26.42
14	50.76	39.78	26.42
15	50.76	39.78	26.42
16	50.76	39.78	26.42
17	50.76	39.78	26.42

## 2.4. Characterization of liposomes

### 2.4.1. Particle morphology, mean vesicle size, and zeta potential

The prepared NSD-LPs were characterized for their morphology, mean vesicle size, and zeta potential. The NSD-LPs were examined using the inverted microscope (Olympus IX53, Japan) using an oil-immersion lens at 2000 x and 3000 x for assessing the morphology of LPs. Further, the mean vesicle size and zeta potential were characterized using Horiba SZ-100 for NSD-LPs. The sample was diluted 10-fold by employing double-distilled water and was sonicated for 10 minutes. The sample was inserted into a cuvette and subsequently placed into a DLS analyser. Measurements of particle sizes and Zeta potential were then recorded. The zeta potential of the excipients was also recorded to compare it with the zeta potential of the final formulation.

### 2.4.2. Percentage entrapment efficiency and drug loading capacity

The prepared liposomes were evaluated for entrapment efficiency (%) and loading capacity (%) using the reported method (Cheng et al., 2019; Dave et al., 2025). Briefly, the LP dispersion (0.1 mL) was dissolved using methanol (10 mL), then the dispersion was centrifuged for 90 min at 4°C at 14,000 rpm (Cooling microcentrifuge; Sorvall Legend X1; ThermoScientific; USA). The supernatant was taken out, and after appropriate dilution, the

unentrapped drug was measured by UV-Vis spectrophotometer (UV-1800, Shimadzu Corporation, Kyoto, Japan) method at 332 nm; HSPC, soyabean oil, and cholesterol interaction was subtracted using blank formulations. Entrapment efficiency and loading capacity were calculated employing the following equation:

$$\text{Entrapment efficiency (\%)} = \frac{\text{Concentration of drug in Liposomes}}{\text{Concentration of Drug used in Formulation}} \times 100 \dots \dots \dots (2)$$

$$\text{Loading Capacity (\%)} = \frac{\text{Concentration of drug in Liposomes}}{\text{Total Concentration of Drug and lipids}} \times 100 \dots \dots \dots (3)$$

#### 2.4.3. Fourier-transform infrared spectroscopy study

The potential drug interaction after incorporation in the formulation was evaluated using Fourier-Transform Infrared Spectroscopy (FTIR) analysis (Cary-630, Agilent). Concisely, the samples were scanned from  $4000\text{ cm}^{-1}$  to  $500\text{cm}^{-1}$ . Both the NSD pure drug and its Liposomal dispersion were characterized simultaneously using the same process and conditions.

#### 2.4.4 Powder X-ray diffraction analysis

A physical examination utilizing X-ray diffraction (XRD) of pure NSD and lyophilized NSD-LPs was conducted to confirm potential interactions between drugs and carriers. The scans were performed with a zero backdrop to simplify the process. The diffraction patterns were obtained by utilizing an X-ray diffractometer (Bruker D8 Advance, Karlsruhe, Germany) furnished with  $\text{Cu-K}\alpha$  radiation ( $\lambda = 1.54\text{ \AA}$ ) operating at 40 kV. The diffraction angle ( $2\theta$ ) was incrementally scanned with  $0.02^\circ$  intervals from  $5$  to  $60^\circ$  at a rate of 1 s/step.

#### 2.4.5. Compatibility via thermal analysis

Differential scanning calorimetry (DSC) is utilized to examine the changes in enthalpy and entropy caused by differences in heat and time in the physiological and biochemical features of a substance. The DSC thermograms of pure NSD and NSD-LPs were generated to check the thermal behaviour of the formulation in comparison with the pure drug. The freshly developed liposomes and lyophilized samples of liposome after reconstitution were sealed in aluminium pans and heated in the differential scanning calorimeter (Mettler-Toledo, GmbH, Switzerland), from  $20$  to  $400\text{ }^\circ\text{C}$ , at a rate of  $10\text{ }^\circ\text{C}/\text{min}$ , under a nitrogen purge flow of  $50\text{ mL}/\text{minute}$ , by employing an empty aluminium pan as a reference. The phase transition temperature ( $T_m$ ) was determined as the midpoint of the transition for all the formulations.

### 2.5. In-vitro dissolution

The *in-vitro* release of NSD from NSD-LPs compared with plain NSD suspension was investigated by employing the dialysis bag technique. The USP type II (paddle) (Electrolab Inspire, Mumbai, India) device is utilized for the purpose of dissolution. A  $100\text{ mL}$  volume of phosphate buffer ( $\text{pH } 7.4$ ) was poured into the dissolution vessels, and for greater specificity, dialysis tubes (molecular weight cutoff: 12000 Da) have been incorporated with NSD at a concentration of  $5\text{ mg}$ . LP dispersion, equivalent to  $5\text{ mg}$ , has been prepared based on the EE (%). The dialysis bags were tightly fastened using paddles and submerged in vessels filled with a dissolution medium. The dissolution conditions were kept constant at a temperature of  $37\text{ }^\circ\text{C}$ . The paddle's rotation speed was set to 100

rpm at particular time intervals (0.5, 1, 2, 4, 6, 8, 12, 24, 48 h). Three mL of media was collected, and fresh volume was added to ensure the sink conditions. The analysis of each sample was done by using a UV-visible spectrophotometer at a wavelength of 332 nm (n=3). The relationship between release behaviour and time was graphed, with the data presented as a percentage of the total drug release.

## 2.6. Lyophilization of optimized LPs

The freeze-drying of NSD-LPs was conducted utilizing VirTis AdVantage PLUS equipment (SP Scientific). In this, one mL of liposomal solution was deposited into glass vials, which were then positioned on the shelf within the apparatus. The LP dispersion consisted of 5 % sucrose, which serves as a cryoprotectant. This is followed by lowering the shelf temperature and sustained at -40 °C, whereas the 100 mbars of chamber pressure was set for 145 min to enable the complete freezing of the LPs. For the sublimation of solvent, it was subjected to reduced pressure up to 150 mbars and elevating the temperature up to 30 °C for a duration of 23 h and 20 min. The secondary drying was conducted to eliminate absorbed water from the product. For achieving this, the shelf temperature was elevated and kept at 20° C for almost 20 h. Upon completion of the procedure, the vials were sealed with rubber closures and kept at 4 °C until subsequent analysis.

## 2.7. Stability Study

An investigation of the stability of NSD-LPs. The formulation was also kept under refrigeration at a temperature range of 2-8 °C. The batch that was manufactured underwent testing for EE (%) after 1 month, 3 months, and 6 months using UV-Vis spectrophotometry.

## 3. Results and Discussion

### 3.1. Experimental design

According to the 3 levels specified in Table 1, Design Expert software generated a total of 17 trial batches. The optimization of batches was performed based on the percentage of drug content and the size of the vesicles. A BBD (Box-Behnken design) with three factors and three levels was used to optimize the characteristics of the liposomal formulation. In summary, three separate variables were chosen, as indicated in **Tables 1 and 2**. Seventeen batches of NSD-LPs were produced using the thin film hydration process (Table 3). Subsequently, the gathered data of the response variable were analysed and provided valuable information as the statistical framework for statistical analysis. Afterwards, the variables and different answers were examined to derive a quadratic polynomial model.

The ANOVA findings specified that the quadratic model had a significant effect ( $p<0.05$ ) on the design. The adjusted  $R^2$  values, specifically 0.9674 for drug content and 0.9643 for vesicle size, were obtained. These values indicate that the produced polynomials were highly accurate and statistically significant at the  $p<0.05$  level. The 2D and 3D graphs are derived from the analysis of DoE data and are utilized to monitor and identify the influential independent variables for a given response. These graphs demonstrate the influence of each variable on each response, which may be observed using the formulated models. The generated plots were carefully examined to assess the direct impact and interplay among factors, which were crucial and taken into account for the selection of the experimental model (**Fig.1**).

### 3.1.1. Influence of input variables on drug content

The equation presents the regression coefficient that represents the overall influence of different factors on drug content. The regression coefficient in the equation indicated the extent of the effect of the concentration of the independent factor on the response, with positive and negative signs, respectively. **Fig. 1 (A and B)** displays the 3D response surfaces and contour plots illustrating the impact of input variables on drug content. The selected variables have a major impact on the drug content. The linear model for drug content showed a statistically significant result with  $p < 0.05$ . Additionally, there was a minimal difference seen between the adjusted R-squared value (0.9674) and the predicted R-squared value (0.9577). This indicates a strong correlation between the experimental and projected findings. The signal-to-noise ratio, calculated with a high level of precision ( $32.98 > 4$ ), indicates that there are sufficient signals to guide the exploration of the design space. The response graph slope indicates that increasing the ratio of enhanced lipid (HSPC) to cholesterol leads to an increase in the value of drug content. Conversely, the ratios of CHOL to soybean oil and lipid to soybean oil demonstrated a decrease in the value of drug content.

### 3.1.2. Influence of input variables on mean vesicle size

The polynomial equation provides a concise representation of the impact of specific parameters on vesicle size, using a recommended quadratic model. The model was deemed significant based on its higher F-value of 48.96, indicating a minimal likelihood of error. The model demonstrated a strong agreement, as indicated by a high  $R^2$  value of 0.9844. Once again, there was a little discrepancy between the values of predicted  $R^2$  (0.9573) and adjusted  $R^2$  (0.9643), indicating that the chosen model is appropriate for subsequent exploration of the design space. **Fig. 1 (C and D)** depicts 3-D surface and contour plots illustrating the percentage of drug content. The graphs indicate that a low percentage of drug content can be attained by using a high Lipid: cholesterol ratio. Additionally, a high percentage of drug content can be obtained by using the CHOL: soybean oil and soybean oil: lipid ratios, which are favourable for achieving high drug content.

**Table 3.** Design matrix for BBD for NSD-LPs.

Run	X1	X2	X3	Y1		Y2	
	Lipid (mg)	Cholesterol (mg)	Soyabean oil (mg)	Drug content (%)		Vesicle size (nm)	
				Actual	Predicted	Actual	Predicted
1	33.25	8.65	26.42	74.71±1.24	76.82	153.5±1.54	158.19
2	68.26	8.65	26.42	77.61±2.52	77.78	164.5±2.41	157.64
3	33.25	70.91	26.42	74.91±1.43	77.05	153.4±1.47	160.26

4	68.26	70.91	26.42	77.23±2.64	78.01	164.7±2.41	160.01
5	33.25	39.78	5.58	77.13±2.51	77.26	168.3±2.19	170.63
6	68.26	39.78	5.58	77.84±2.45	77.41	166.2±1.09	166.78
7	33.25	39.78	47.26	79.73±2.17	76.61	188.2±1.81	174.31
8	68.26	39.78	47.26	77.63±1.64	77.57	166.4±2.51	164.06
9	50.76	8.65	5.58	79.72±1.81	77.63	186.1±1.18	179.07
10	50.76	70.91	5.58	79.91±1.38	77.85	187.2±1.84	178.00
11	50.76	8.65	47.26	76.88±1.24	76.98	160.4±2.24	169.59
12	50.76	70.91	47.26	77.77±2.26	77.20	168.1±2.47	175.12
13	50.76	39.78	26.42	77.86±2.34	77.41	167.1±2.41	166.78
14	50.76	39.78	26.42	77.84±2.12	78.22	166.2±2.14	166.78
15	50.76	39.78	26.42	74.83±2.27	77.41	154.2±1.48	166.78
16	50.76	39.78	26.42	74.91±1.32	77.41	159.3±2.34	166.78
17	50.76	39.78	26.42	79.54±2.07	77.41	187.1±1.29	166.78

Values indicated as mean ± SD, n = 3

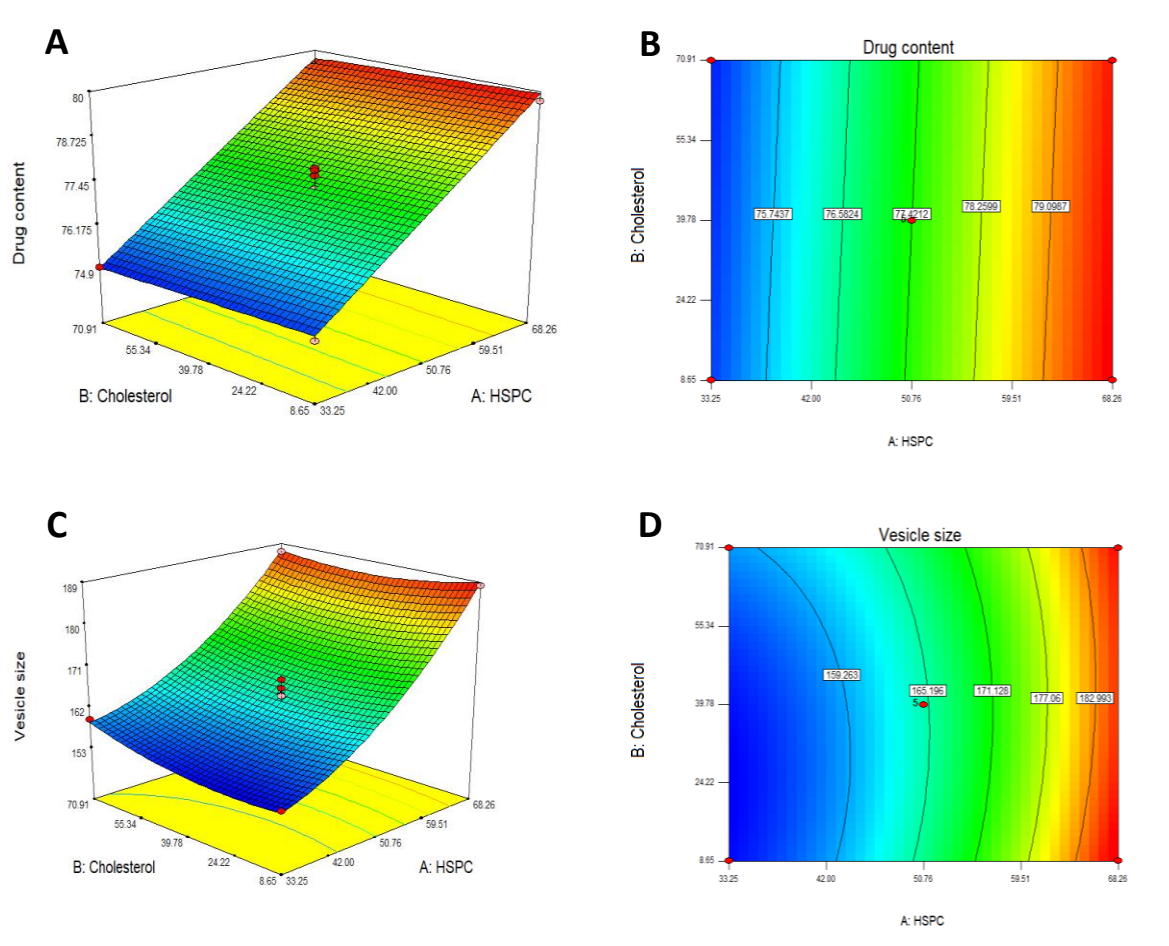


**Figure 1.** 3D (A and C) and Contour plots (B and D) showing the effect of input variables on % drug content and vesicle size.

### 3.2. Optimization and validation of NSD-LPs

The estimation of optimized formulation was based on maximizing drug content and minimizing vesicle size of NSD-LPs. The desirability approach revealed the best composition of 68.26 mg of HSPC, 70.91 mg of Cholesterol, and 5.58 mg of Soyabean oil with high desirability (0.631). The predicted values of responses were 78.33 % of drug content and 168.29 nm of vesicle size. The optimized formulation was prepared according to the suggested solution, and actual values were observed values with 80.94 % of drug content and 149.2 nm vesicle size, showing agreement with predicted values. The outcomes of the experimental design highlighted the applicability and efficiency of using BBD for this experimental setting in developing LPs with desired properties.

### 3.3. Characterization of optimized liposomes

#### 3.3.1. Particle morphology, mean vesicle size analysis, and zeta potential

The liposomes loaded with NSD exhibited an average particle size of 149.2 nm, as determined by **Fig. 2 (A)**. The polydispersity index (PDI) was measured to be 0.261, indicating that NSD-LPs exhibit monodispersity, suggesting that they have a uniform size. **Fig. 2 (B)** demonstrates the zeta potential of liposomes loaded with NSD. The LPs

displayed a negative zeta potential of (- mV), suggesting their anionic nature. Prior studies have determined that poly-anions exhibit superior bio-adhesive potency in comparison with poly-cations (Dusane et al., 2010; Lin et al., 2017). The liposomes were found to possess a negative zeta potential, which suggests that they exhibit more stability. The zeta potential of NSD-LPs was determined to be -14.2 mV (**Fig. 2 (B)**). Additionally, the zeta potential of HSPC ( $-5.8 \pm 0.4$ ), cholesterol ( $-2.1 \pm 0.3$ ), soybean oil ( $-6.3 \pm 0.5$ ), and rhamnolipid ( $-24.8 \pm 1.1$ ) were determined, wherein the rhamnolipid demonstrated the most negative potential, whereas HSPC, cholesterol, and soybean oil exhibited mild negative charges. It confirms that the distinct negative charge of the formulations was mainly due to the presence of rhamnolipid. **Fig.2 (C) and (D)** indicate homogeneously dispersed, spherical droplets without showing any aggregation, suggesting appropriate colloidal stability of the nanoemulsion system.

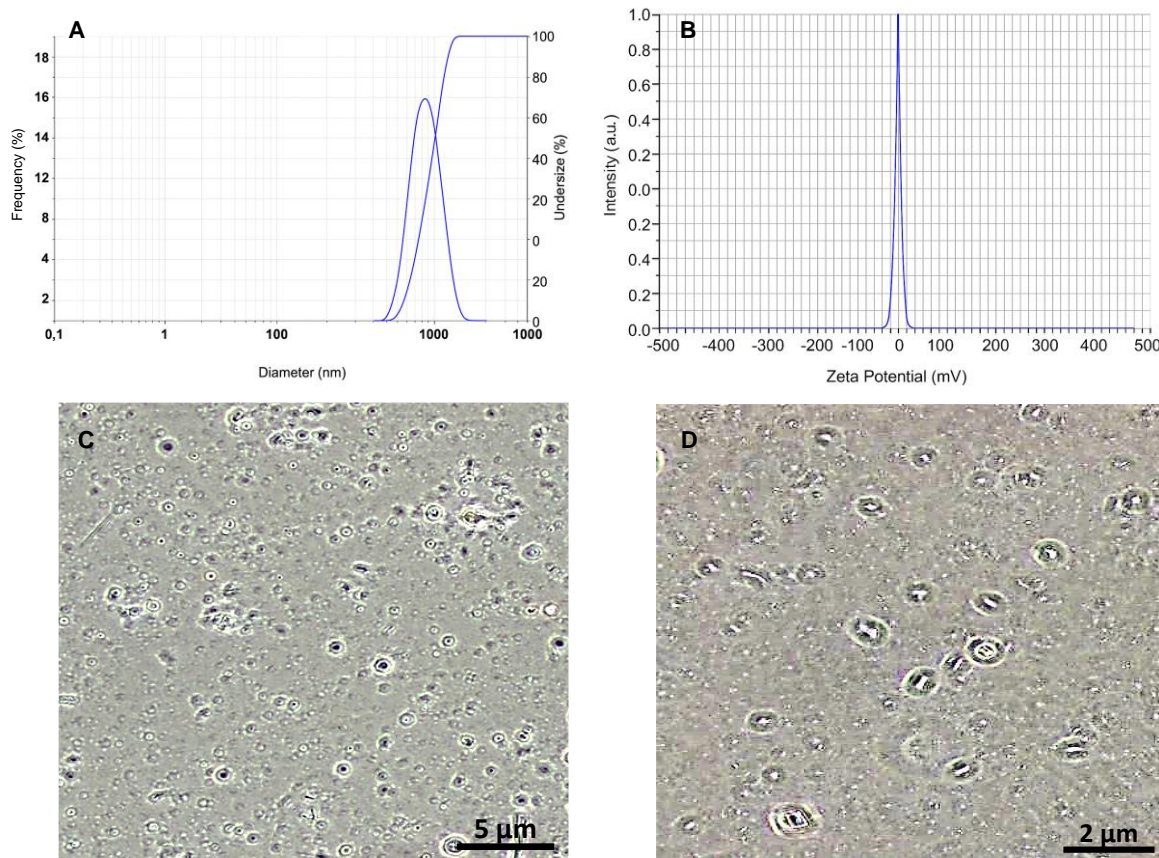


**Figure 2.** Size distribution of mean vesicle size (A), zeta potential (B), microscopic images of vesicles at 5  $\mu$ m (C) and 2  $\mu$ m (D), of NSD-LPs.

### 3.3.2. Fourier-transform infrared spectroscopy study

All the functional group peaks corresponding to the respective functional group present in the NSD are present in the FTIR spectrum. **Fig. 3 (A and B)** comprises FTIR spectra showing functional groups present in the NSD structure, which indicates the drug is pure and it not undergone any functional group modifications. In NSD-LPs, all the stretching frequencies are retained as reported, which indicates that the loaded NSD retained its integrity in liposomes. Furthermore, the pure NSD spectrum demonstrated unique N–H stretching ( $\sim 3310 \text{ cm}^{-1}$ ), aliphatic C–H stretching ( $\sim 2897 \text{ cm}^{-1}$ ), amide/aryl C=O, and C=C stretching ( $\sim 1679\text{--}1559 \text{ cm}^{-1}$ ), and bending of aromatic ring ( $\sim 731 \text{ cm}^{-1}$ ), indicating the presence of the distinct functional groups (Real et al., 2023; Vazquez-Rodriguez

et al., 2022). In the NSD-LP spectrum, the appearance of these slightly broader peaks is minimized, and minimized intensity is minimized after encapsulation within the lipid bilayer. However, there were no observations of new peaks or loss of significant NSD peaks, indicating the absence of chemical interactions or degradation. The slight peak shifting displayed consistently along with non-covalent interactions between NSD and the lipid components (Caldas et al., 2021; Jiang et al., 2024; *Liposomes: A Practical Approach*, 2003).

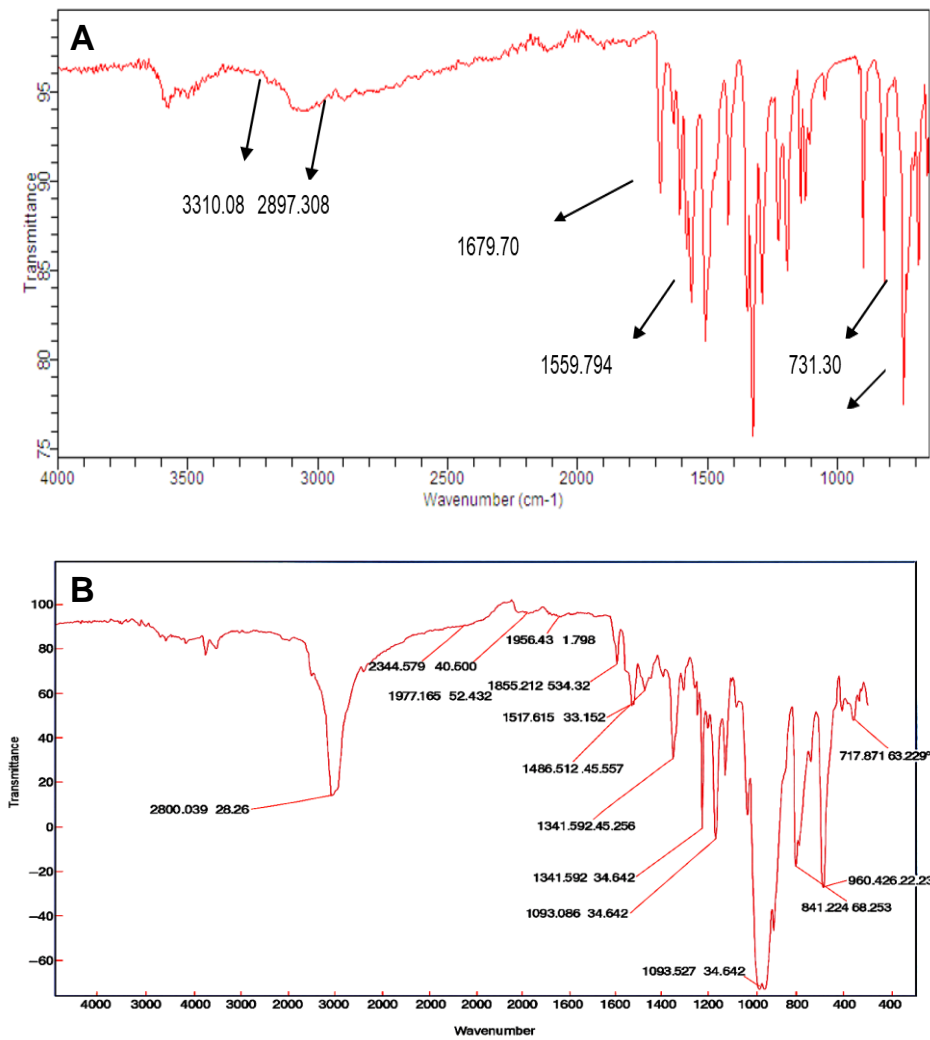


**Figure 3.** FTIR spectra of Pure NSD (A) and NSD-LPs (B).

### 3.3.3. Powder XRD analysis

XRD has been extensively utilized for the analysis of nanoparticles to accurately determine important characteristics, including crystal structure, crystallite size, and strain. The widening of diffraction peaks is a result of the presence of disordered states within crystals. The diffraction patterns of both the pure drug and NSD-LPs samples are displayed in **Fig. 4 (A and B)**. The NSD XRD pattern displayed clear and prominent high-energy diffraction peaks, indicating the crystalline nature of the NSDs. The XRD patterns of lyophilized NSD-LPs exhibited characteristic high-energy diffraction patterns, indicating that the formulation was in an amorphous state.

The crystalline diffractions of pure NSD were observed in accordance with previous studies with peaks at approximately 6.7°, 13.1°, 17.3°, 19.8°, 22.3°, and 25.6° (2θ), therefore validating the identification and crystallinity of the drug (Baek et al., 2024; Guo et al., 2015). Contrarily, the absence or reduction of these peaks in NSD liposomes corresponds well to previously reported studies demonstrating that encapsulation results in partial amorphization and molecular dispersion of NSD within lipid or polymer matrix systems. Furthermore, the lipid excipients like phospholipids and cholesterol are recognized to generate halo-like amorphous patterns that conceal drug peaks when the drug is molecularly dispersed (Naqvi et al., 2017; Tai et al., 2025; Wdowiak et al., 2024).

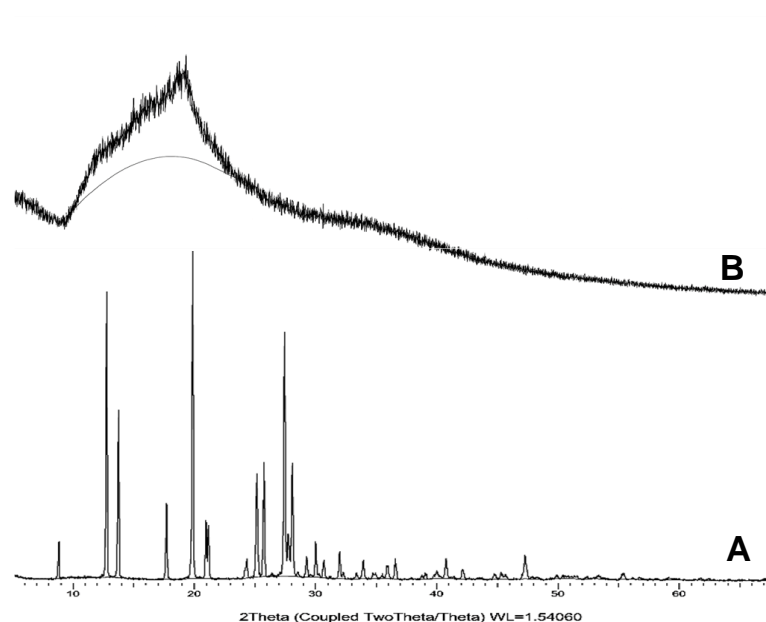


**Figure 4.** XRD pattern of pure NSD (A), and Optimized NSD-LPs (B).

### 3.3.4. Compatibility via thermal analysis

The DSC thermograms of pure NSD and its formulation in a dry inert nitrogen atmosphere are shown in **Fig. 5A**. The DSC thermogram displayed a prominent peak at around 225 °C, which corresponds to NSD. The distinct endothermic transition verifies the crystalline nature of pure NSD, which was in accordance with the reported melting range of 220 to 230 °C (Rehman et al., 2018; Sanphui et al., 2012). Contrarily, the optimized NSD-LPs (**Fig. 5B**) demonstrated a broader and lowered intensity thermal event, possibly due to conversion of NSD into a molecular dispersion or partial amorphization within the lipid matrix. This loss in crystallinity usually shows effective encapsulation and disruption of drug lattice structure in the phospholipid vesicles (Li et al., 2017; Verma et al., 2025). The melting temperature peak of the NSD reduced after being encapsulated in NSD-LPs, suggesting a disrupted crystalline structure and uneven distribution of molecules inside the polymer matrix.

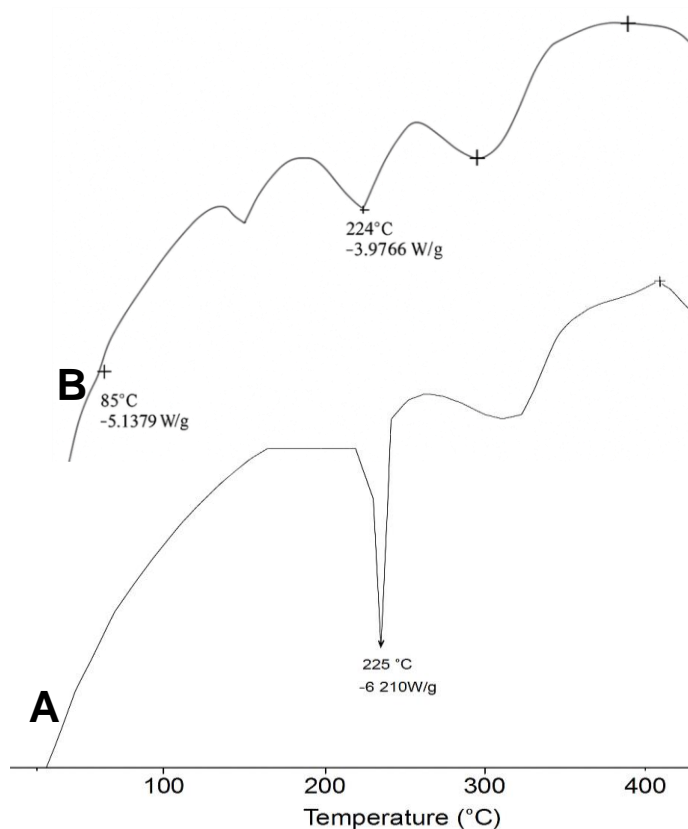


**Figure 5.** DSC thermogram of pure NSD (A), and Optimized NSD-LPs (B).

### 3.4. In vitro drug release

The drug release profile of plain NSD and NSD-LPs showed a distinct release pattern, indicating the effect of the liposomal entrapment on the release kinetics (Fig. 6). The plain NSD demonstrated a faster dissolution behaviour, with more than 95 % release of drug within 8 h, indicating almost complete release in a comparatively short duration. This can be attributed to the instantaneous solubilization of the free drug in the release medium with no signs of any physical or chemical barriers to diffusion. Contrarily, the NSD-LPs formulation exhibited a substantial sustained release profile, with ~30% of NSD release in the first 8 h, and a slow increment in release over the study period. The entrapment of NSD within the phospholipid bilayer of LPs formulation, which played the role of a diffusion barrier, contributed to controlled drug release into the media. Furthermore, the drug release may have been slowed owing to the amphiphilic nature of the liposomal membranes and probable interactions between the drug and lipid. Such a sustained release feature of NSD-LPs is beneficial for ensuring extended therapeutic drug concentrations at the target site, possibly may enhance bioavailability of the drug, and lower dosing frequency in comparison with pure NSD (Gkionis et al., 2021; Sobol et al., 2025).

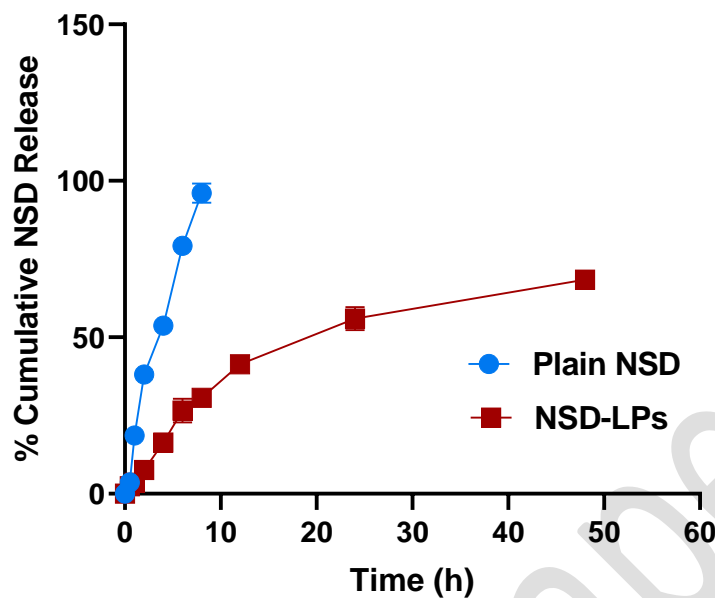


**Figure 6.** Percentage cumulative NSD release of plain NSD and Optimized NSD-LPs (Mean± S.D., n=3)

### 3.5. Stability Study

The stability of NSD-LPs formulation was determined by checking entrapment efficiency for 6 months, and the NSD content was determined using the utilization of UV-visible spectroscopy at a wavelength of 232 nm. The NSD batch, which has been prepared, has consistent outcomes after 1 month, 3 months, and 6 months. Therefore, this formulation exhibited stability, and the outcomes are displayed in Table 4.

**Table 4.** Outcomes of the stability study of Optimized NSD-LPs formulation.

Entrapment efficiency (%)			
0 month	1month	3 months	6 months
57.31±1.86	53.2 ± 1.41	50.21 ± 1.88	48.28 2.35

### 4. Conclusion

NSD-LPs modified with rhamnolipids were successfully developed and optimized employing a Box-Behnken Design approach. The optimized formulation exhibited high drug content, nanometric vesicle size, homogeneous dispersion, and negative zeta potential, contributing to the stability of the formulation. The structural and thermal studies verified effective entrapment of NSD with no signs of compromised molecular interactions. The *in vitro* release studies exhibited a sustained release behaviour, which may eventually contribute to improving bioavailability and possibly lowering dosing frequency. The stability studies showed that the formulation retained its physicochemical features for a 6-month study period. Conclusively, the reported delivery systems propose an exciting approach for dealing with the solubility of drugs, which opens up the path for future *in vivo* studies and

clinical translation. However, the formulation displayed promising physicochemical features and sustained *in vitro* release characteristics, but the current study has specific limitations. The *in vivo* pharmacokinetic and biodistribution studies are needed to verify its therapeutic effectiveness. Additionally, the long-term stability study, regulatory considerations, and scale-up possibility still need to be explored in future work to facilitate efficient clinical translation.

#### **Credit authorship contributions statement**

Sujit A Desai and Sudarshan Singh: Conceptualization, writing original draft, writing review and editing; Himanshu Paliwal, Sachin S Mali, Anbhule Sachin Jalindar, and Arehalli Manjappa: methodology, writing original draft, writing review and editing; Durgacharan A Bhagwat and Bhupendra G. Prajapati: Formal analysis and Validation

#### **Acknowledgments**

This work was partially supported by CMU Proactive Researcher Scheme (2023), Chiang Mai University.

#### **Declaration of generative AI and AI-assisted technologies in the writing process**

No AI or AI-based software has been used in either writing, editing, or correction of manuscript.

#### **Funding information**

This work did not receive funding from any agency.

#### **Declaration of Competing Interest**

The authors declare that there is no known conflict of interest.

#### **Data availability statement**

The data can be made available on request to the corresponding authors.

#### **References**

Al-Gareeb, A. I., Aljubory, K. D., & Alkuraishy, H. M. (2017). Niclosamide as an anti-obesity drug: an experimental study. *Eating and Weight Disorders-Studies on Anorexia, Bulimia and Obesity*, 22(2), 339-344.

Baek, K., Woo, M. R., Ud Din, F., Choi, Y. S., Kang, M. J., Kim, J. O., Choi, H. G., & Jin, S. G. (2024). Comparison of Solid Self-Nanoemulsifying Systems and Surface-Coated Microspheres: Improving Oral Bioavailability of Niclosamide. *International Journal of Nanomedicine*, 19, 13857-13874. <https://doi.org/10.2147/ijn.S494083>

Bhalani, D. V., Nutan, B., Kumar, A., & Singh Chandel, A. K. (2022). Bioavailability enhancement techniques for poorly aqueous soluble drugs and therapeutics. *Biomedicines*, 10(9), 2055.

Caldas, A. R., Catita, J., Machado, R., Ribeiro, A., Cerqueira, F., Horta, B., Medeiros, R., Lúcio, M., & Lopes, C. M. (2021). Omega-3- and Resveratrol-Loaded Lipid Nanosystems for Potential Use as Topical Formulations in Autoimmune, Inflammatory, and Cancerous Skin Diseases. *Pharmaceutics*, 13(8), 1202. <https://www.mdpi.com/1999-4923/13/8/1202>

Chen, H., Yang, Z., Ding, C., Chu, L., Zhang, Y., Terry, K., Liu, H., Shen, Q., & Zhou, J. (2013). Discovery of O-alkylamino-tethered niclosamide derivatives as potent and orally bioavailable anticancer agents. *ACS medicinal chemistry letters*, 4(2), 180-185.

Cheng, C., Wu, Z., McClements, D. J., Zou, L., Peng, S., Zhou, W., & Liu, W. (2019). Improvement on stability, loading capacity and sustained release of rhamnolipids modified curcumin liposomes. *Colloids and Surfaces B: Biointerfaces*, 183, 110460.

Das, P., Mukherjee, S., & Sen, R. (2008). Genetic regulations of the biosynthesis of microbial surfactants: an overview. *Biotechnology and Genetic Engineering Reviews*, 25(1), 165-186.

Dave, J., Jani, H., Patel, Y., Mohite, P., Puri, A., Chidrawar, V. R., Datta, D., Bandi, S. P., Ranch, K., & Singh, S. (2025). Polyol-modified deformable liposomes fortified contact lenses for improved ocular permeability. *Nanomedicine*, 20(7), 649-662.

Dusane, D. H., Nancharaiah, Y. V., Zinjarde, S. S., & Venugopalan, V. P. (2010). Rhamnolipid mediated disruption of marine *Bacillus pumilus* biofilms. *Colloids and Surfaces B: Biointerfaces*, 81(1), 242-248. <https://doi.org/https://doi.org/10.1016/j.colsurfb.2010.07.013>

Fan, X., Li, H., Ding, X., & Zhang, Q.-Y. (2019). Contributions of hepatic and intestinal metabolism to the disposition of niclosamide, a repurposed drug with poor bioavailability. *Drug Metabolism and Disposition*, 47(7), 756-763.

Gkionis, L., Aojula, H., Harris, L. K., & Tirella, A. (2021). Microfluidic-assisted fabrication of phosphatidylcholine-based liposomes for controlled drug delivery of chemotherapeutics. *International Journal of Pharmaceutics*, 604, 120711. <https://doi.org/https://doi.org/10.1016/j.ijpharm.2021.120711>

Guo, L. Q., Xu, K. L., Ma, X. L., Li, S. S., & Li, H. (2015). X-ray powder diffraction data for niclosamide, C13H8N2O4Cl2. *Powder Diffraction*, 30(4), 375-377. <https://doi.org/10.1017/S0885715615000615>

Haba, E., Bouhdid, S., Torrego-Solana, N., Marqués, A., Espuny, M. J., García-Celma, M. J., & Manresa, A. (2014). Rhamnolipids as emulsifying agents for essential oil formulations: antimicrobial effect against *Candida albicans* and methicillin-resistant *Staphylococcus aureus*. *International Journal of Pharmaceutics*, 476(1-2), 134-141.

He, X., Li, M., Ye, W., & Zhou, W. (2021). Discovery of degradable niclosamide derivatives able to specially inhibit small cell lung cancer (SCLC). *Bioorganic Chemistry*, 107, 104574.

Hsu, C.-Y., Mahmoud, Z. H., Hussein, U. A.-R., Abduvalieva, D., Alsultany, F. H., & Kianfar, E. (2025). Biosurfactants: Properties, applications and emerging trends. *South African Journal of Chemical Engineering*, 53, 21-39. <https://doi.org/https://doi.org/10.1016/j.sajce.2025.04.002>

Isailović, B. D., Kostić, I. T., Zvonar, A., Đorđević, V. B., Gašperlin, M., Nedović, V. A., & Bugarski, B. M. (2013). Resveratrol loaded liposomes produced by different techniques. *Innovative Food Science & Emerging Technologies*, 19, 181-189. <https://doi.org/https://doi.org/10.1016/j;ifset.2013.03.006>

Jain, N. K., Prabhuraj, R., Bavya, M., Prasad, R., Bandyopadhyaya, R., Naidu, V., & Srivastava, R. (2019). Niclosamide encapsulated polymeric nanocarriers for targeted cancer therapy. *RSC Advances*, 9(46), 26572-26581.

Jangde, R., & Singh, D. (2016). Preparation and optimization of quercetin-loaded liposomes for wound healing, using response surface methodology. *Artificial Cells, Nanomedicine, and Biotechnology*, 44(2), 635-641. <https://doi.org/10.3109/21691401.2014.975238>

Jiang, Y., Li, W., Wang, Z., & Lu, J. (2024). Lipid-Based Nanotechnology: Liposome. *Pharmaceutics*, 16(1), 34. <https://www.mdpi.com/1999-4923/16/1/34>

Ju, C., & Zhang, C. (2021). Preparation and Characterization of pH Sensitive Drug Liposomes. In *Liposome-Based Drug Delivery Systems* (pp. 385-408). Springer.

Kosaric, N., & Sukan, F. V. (2014). Biosurfactants: Production and Utilization-Processes, Technologies, and Economics.

Li, Z., Zhang, M., Liu, C., Zhou, S., Zhang, W., Wang, T., Zhou, M., Liu, X., Wang, Y., Sun, Y., & Sun, J. (2017). Development of Liposome containing sodium deoxycholate to enhance oral bioavailability of itraconazole. *Asian Journal of Pharmaceutical Sciences*, 12(2), 157-164. <https://doi.org/https://doi.org/10.1016/j.ajps.2016.05.006>

Lin, W., Liu, S., Tong, L., Zhang, Y., Yang, J., Liu, W., Guo, C., Xie, Y., Lu, G., & Dang, Z. (2017). Effects of rhamnolipids on the cell surface characteristics of *Sphingomonas* sp. GY2B and the biodegradation of phenanthrene [10.1039/C7RA02576A]. *RSC Advances*, 7(39), 24321-24330. <https://doi.org/10.1039/C7RA02576A>

*Liposomes: A Practical Approach.* (2003). Oxford University Press. <https://doi.org/10.1093/oso/9780199636556.001.0001>

Lodagekar, A., Borkar, R. M., Thatikonda, S., Chavan, R. B., Naidu, V., Shastri, N. R., Srinivas, R., & Chella, N. (2019). Formulation and evaluation of cyclodextrin complexes for improved anticancer activity of repurposed drug: Niclosamide. *Carbohydrate Polymers*, 212, 252-259.

Lourith, N., & Kanlayavattanakul, M. (2009). Natural surfactants used in cosmetics: glycolipids. *International journal of cosmetic science*, 31(4), 255-261.

Luo, D., Carter, K. A., Molins, E. A., Straubinger, N. L., Geng, J., Shao, S., Jusko, W. J., Straubinger, R. M., & Lovell, J. F. (2019). Pharmacokinetics and pharmacodynamics of liposomal chemophototherapy with short drug-light intervals. *Journal of Controlled Release*, 297, 39-47.

Mali, S. S., Singh, S., Patil, R. R., & Patil, P. R. (2025). Bridging Innovation: Exploring the Versatility of Value-added Biosurfactants Across Diverse Applications.

Mast, M.-P., Modh, H., Knoll, J., Fecioru, E., & Wacker, M. G. (2021). An update to dialysis-based drug release testing—data analysis and validation using the pharma test dispersion releaser. *Pharmaceutics*, 13(12), 2007.

Mito, S., Cheng, B., Garcia, B. A., Ooi, X. Y., Gonzalez, D., Ruiz, T. C., Elisarraras, F. X., & Tsin, A. (2023). SAR study of niclosamide derivatives for neuroprotective function in SH-SY5Y neuroblastoma. *Bioorganic & Medicinal Chemistry Letters*, 96, 129498.

Mohite, P., Puri, A., Bharati, D., Munde, S., Malhan, A., Guleria, M., Datta, D., Pawar, A., Ranch, K., Singh, S., & Kausar, N. (2025). Demystifying the Potential of Polymeric Lipids as Substitute in Regenerative Applications: A Review. *Polymers for Advanced Technologies*, 36(2), e70096. <https://doi.org/https://doi.org/10.1002/pat.70096>

Mohite, P., Singh, S., Pawar, A., Sangale, A., & Prajapati, B. G. (2023). Lipid-based oral formulation in capsules to improve the delivery of poorly water-soluble drugs. *Frontiers in Drug Delivery*, 3, 1232012.

Moussa, Z., Chebl, M., & Patra, D. (2017). Interaction of curcumin with 1, 2-dioctadecanoyl-sn-glycero-3-phosphocholine liposomes: Intercalation of rhamnolipids enhances membrane fluidity, permeability and stability of drug molecule. *Colloids and Surfaces B: Biointerfaces*, 149, 30-37.

Müller, F., Hönzke, S., Luthardt, W.-O., Wong, E. L., Unbehauen, M., Bauer, J., Haag, R., Hedtrich, S., Rühl, E., & Rademann, J. (2017). Rhamnolipids form drug-loaded nanoparticles for dermal drug delivery. *European Journal of Pharmaceutics and Biopharmaceutics*, 116, 31-37.

Mulligan, C. N. (2009). Recent advances in the environmental applications of biosurfactants. *Current Opinion in Colloid & Interface Science*, 14(5), 372-378.

Naqvi, S., Mohiyuddin, S., & Gopinath, P. (2017). Niclosamide loaded biodegradable chitosan nanocargoes: an *<sup>i</sup>in vitro* study for potential application in cancer therapy. *Royal Society Open Science*, 4(11), 170611. <https://doi.org/doi:10.1098/rsos.170611>

Nassir, F., & Ibdah, J. A. (2014). Role of mitochondria in nonalcoholic fatty liver disease. *International Journal of Molecular Sciences*, 15(5), 8713-8742.

Nitschke, M., & Costa, S. (2007). Biosurfactants in food industry. *Trends in Food Science & Technology*, 18(5), 252-259.

Panchal, K., Patel, Y., Jani, H., Dalal, M., Chidrawar, V. R., Datta, D., Mohite, P., Puri, A., Ranch, K., & Singh, S. (2025). Indomethacin-incorporated microemulsion-laden contact lenses for improved ocular drug delivery and therapeutic efficacy [10.1039/D5RA01046B]. *RSC Advances*, 15(20), 16110-16124. <https://doi.org/10.1039/D5RA01046B>

Plaza-Oliver, M., Santander-Ortega, M. J., & Lozano, M. V. (2021). Current approaches in lipid-based nanocarriers for oral drug delivery. *Drug Delivery and Translational Research*, 11(2), 471-497. <https://doi.org/10.1007/s13346-021-00908-7>

Real, J. P., Real, D. A., Lopez-Vidal, L., Barrientos, B. A., Bolaños, K., Tinti, M. G., Litterio, N. J., Kogan, M. J., & Palma, S. D. (2023). 3D-Printed Gastroretentive Tablets Loaded with Niclosamide Nanocrystals by the Melting Solidification Printing Process (MESO-PP). *15(5)*, 1387. <https://www.mdpi.com/1999-4923/15/5/1387>

Rehman, M. U., Khan, M. A., Khan, W. S., Shafique, M., & Khan, M. (2018). Fabrication of Niclosamide loaded solid lipid nanoparticles: in vitro characterization and comparative in vivo evaluation. *Artificial Cells, Nanomedicine, and Biotechnology*, 46(8), 1926-1934. <https://doi.org/10.1080/21691401.2017.1396996>

Sachdev, D. P., & Cameotra, S. S. (2013). Biosurfactants in agriculture. *Applied Microbiology and Biotechnology*, 97(3), 1005-1016.

Sanches, B. C. P., Rocha, C. A., Martin Bedoya, J. G., da Silva, V. L., da Silva, P. B., Fusco-Almeida, A. M., Chorilli, M., Contiero, J., Crusca, E., & Marchetto, R. (2021). Rhamnolipid-Based Liposomes as Promising Nano-Carriers for Enhancing the Antibacterial Activity of Peptides Derived from Bacterial Toxin-Antitoxin Systems. *Int J Nanomedicine*, 16, 925-939. <https://doi.org/10.2147/ijn.S283400>

Sanphui, P., Kumar, S. S., & Nangia, A. (2012). Pharmaceutical Cocrystals of Niclosamide. *Crystal Growth & Design*, 12(9), 4588-4599. <https://doi.org/10.1021/cg300784v>

Singh, S., Supaweera, N., Nwabor, O. F., Chaichompo, W., Suksamrarn, A., Chittasupho, C., & Chunglok, W. (2024). Poly (vinyl alcohol)-gelatin-sericin copolymerized film fortified with vesicle-entrapped demethoxycurcumin/bisdemethoxycurcumin for improved stability, antibacterial, anti-inflammatory, and skin tissue regeneration. *International Journal of Biological Macromolecules*, 258, 129071. <https://doi.org/https://doi.org/10.1016/j.ijbiomac.2023.129071>

Singh, S., Supaweera, N., Nwabor, O. F., Yusakul, G., Chaichompo, W., Suksamrarn, A., Panpipat, W., & Chunglok, W. (2024). Polymeric scaffold integrated with nanovesicle-entrapped curcuminoids for enhanced therapeutic efficacy. *Nanomedicine*, 19(14), 1313-1329. <https://doi.org/10.1080/17435889.2024.2347823>

Singh, V., Haque, S., Niwas, R., Srivastava, A., Pasupuleti, M., & Tripathi, C. (2017). Strategies for fermentation medium optimization: an in-depth review. *Frontiers in Microbiology*, 7, 2087.

Sobol, Ź., Chiczewski, R., & Wątróbska-Świetlikowska, D. (2025). Advances in Liposomal Drug Delivery: Multidirectional Perspectives on Overcoming Biological Barriers. *Pharmaceutics*, 17(7), 885. <https://doi.org/10.3390/pharmaceutics17070885>

Tai, Y., Zhang, M., Han, Y., Hu, H., Lin, S., Zhai, F., Tian, M., Song, X., Wan, S., Chen, Y., & Jin, D. (2025). Synthetic niclosamide-loaded controlled-release nanospheres with high solubility and stability exerting multiple effects against Clostridioides difficile [Original Research]. *Frontiers in Microbiology*, 16, 1617631. <https://doi.org/10.3389/fmicb.2025.1617631>

Unnisa, A., Chettupalli, A. K., Alazragi, R. S., Alelwani, W., Bannunah, A. M., Barnawi, J., Amarachinta, P. R., Jandrajupalli, S. B., Elamine, B. A., & Mohamed, O. A. (2023). Nanostructured lipid carriers to enhance the bioavailability and solubility of ranolazine: Statistical optimization and pharmacological evaluations. *Pharmaceutics*, 16(8), 1151.

Vazquez-Rodriguez, J. A., Shaqour, B., Guarch-Pérez, C., Choińska, E., Riool, M., Verleije, B., Beyers, K., Costantini, V. J. A., Święszkowski, W., Zaat, S. A. J., Cos, P., Felici, A., & Ferrari, L. (2022). A Niclosamide-releasing hot-melt extruded catheter prevents *Staphylococcus aureus* experimental biomaterial-associated infection. *Scientific Reports*, 12(1), 12329. <https://doi.org/10.1038/s41598-022-16107-4>

Verma, S., Maurya, P., Saraf, S. K., & Datt, N. (2025). Ameliorative effect of dextrose coated rebamipide liposomes for liver cirrhosis: in vitro and in vivo characterization. *Future Journal of Pharmaceutical Sciences*, 11(1), 71. <https://doi.org/10.1186/s43094-025-00826-2>

Wdowiak, K., Miklaszewski, A., & Cielecka-Piontek, J. (2024). Amorphous Polymer-Phospholipid Solid Dispersions for the Co-Delivery of Curcumin and Piperine Prepared via Hot-Melt Extrusion. 16(8), 999. <https://www.mdpi.com/1999-4923/16/8/999>

Yadav, P., Rastogi, V., & Verma, A. (2020). Application of Box-Behnken design and desirability function in the development and optimization of self-nanoemulsifying drug delivery system for enhanced dissolution of ezetimibe. *Future Journal of Pharmaceutical Sciences*, 6(1), 7.

Yi, G., Son, J., Yoo, J., Park, C., & Koo, H. (2019). Rhamnolipid nanoparticles for in vivo drug delivery and photodynamic therapy. *Nanomedicine: Nanotechnology, Biology and Medicine*, 19, 12-21.



Publisher's note: Eurasia Academic Publishing Group (EAPG) remains neutral with regard to jurisdictional claims in published maps and institutional affiliations.

Open Access This article is licensed under a Creative Commons Attribution-NoDerivatives 4.0 International (CC BY-ND 4.0) licence, which permits copying and redistributing the material in any medium or format for any purpose, even commercially. The licensor cannot revoke these freedoms as long as you follow the licence terms. Under the following terms, you must give appropriate credit, provide a link to the license, and indicate if changes were made. You may do so in any reasonable manner, but not in any way that suggests the licensor endorsed you or your use. If you remix, transform, or build upon the material, you may not distribute the modified material. To view a copy of this license, visit <https://creativecommons.org/licenses/by-nd/4.0/>.